High-Efficiency Operation of Wireless In-Wheel Motor at Low Load Using Intermittent Synchronous Rectification with Improved Transient Stability

Daiki Tajima
Department of Advanced Energy, The University of Tokyo
5-1-5, Kashiwanoha, Kashiwa, Chiba, 227-8561 Japan
Email: tajima.daiki18@ae.k.u-tokyo.ac.jp

Osamu Shimizu
Department of Advanced Energy, The University of Tokyo
5-1-5, Kashiwanoha, Kashiwa, Chiba, 227-8561 Japan
Email: shimizu.osamu@edu.k.u-tokyo.ac.jp

Hiroshi Fujimoto
Department of Advanced Energy, The University of Tokyo
5-1-5, Kashiwanoha, Kashiwa, Chiba, 227-8561 Japan
Email: fujimoto@k.u-tokyo.ac.jp

***Abstract*—The authors' research group invented a Wireless In-Wheel Motor (W-IWM) in order to overcome the low reliability of In-wheel motor's power and signal wires. This system uses Wireless Power Transfer (WPT) via magnetic resonant coupling. In order to control the WPT systems with variable power load such as motor, it is required to achieve high efficiency and transfer power corresponding to the load at any time are required. We have developed W-IWM's control methods to transfer desired power with high efficiency. However, the efficiency in the low power output range still has room for improvement. In this paper, novel control method using the intermittent synchronous rectification is proposed. This method improves the efficiency of the W-IWM system in low power output range by improved transient current. Experiments and simulations verify the effectiveness of the proposed method.**

***Index Terms*—wireless power transfer, magnetic resonant coupling, power flow control, supercapacitor, in-wheel motor**

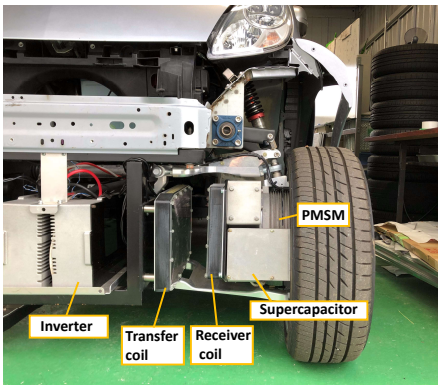

Fig. 1. W-IWM attached to the test vehicle.

I. Introduction

In recent years, electric vehicles (EVs) have attracted attention for their less harmful emissions. Electric vehicles have had the problem of short cruising range so far. Nowadays, in order to solve this problem, research on dynamic wireless power transfer to electric vehicles is in progress [1]. EVs have a very quick torque response provided by motors compared to internal combustion engine vehicles [2]. Moreover, In-wheel motor (IWM)-type EVs have various benefits such as body weight reduction, improvement of body design freedom and independent control of each wheel [3] [4]. However, conventional IWMs have a risk of disconnection of power and signal cables from vehicle body. Those cables are exposed to harsh environment and may became disconnected due to continuous bending, and impacts caused by debris colliding from the road.

To overcome the risk of the disconnection, the authors' research group invented Wireless In-Wheel Motor (W-IWM) in which the IWM receives power without cables [5]. This system employs magnetic resonance coupling as a WPT method since this method is robust to the coil misalignment caused by steering and suspension vibration. In the Wireless Power Transfer (WPT) systems with variable power load such as a motor, the secondary side DC-link voltage is unstable. Then, the transmission power should be controlled to desired power to stabilize the secondary side DC-link voltage.

The control methods for the WPT system under the constant power load have been developed in previous studies. Two-mode control [6] is the simplest method. This method control transmission power by switching rectification mode and short mode of the secondary side converter. In this method, although it is easy to control transmission power, the conduction loss of diode and the loss caused by transient current during mode switching can not be ignored.

In order to reduce those losses, intermittent synchronous rectification was proposed [7]. This method rectifies received current by turning on the SiC MOSFETs instead of SiC diodes and switches between rectification mode and short mode with the zero-crossing of the current. Those features provide low conduction loss.

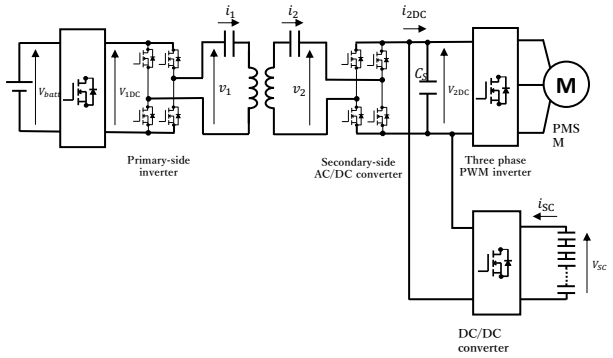

Fig. 2. System configuration of W-IWM2.

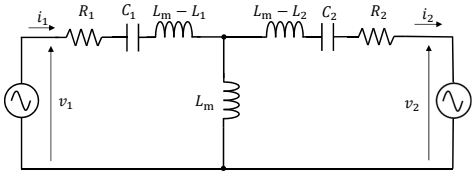

Fig. 3. Equivalent circuit of wireless power transfer via magnetic resonance coupling.

Phase shift control [8] improves the transients by eliminating mode switching. In this method, the PWM duty ratio of 3-level waveform which is the output of the secondary side converter, is manipulated to adjust the transmission power. However, switching loss of the secondary side converter is large especially in the low power output range since the width of the 3-level waveform is thin.

An innovative control method using wheel side supercapacitor is proposed [9]. In the second-generation W-IWM (W-IWM2), a supercapacitor is attached as a power compensator. The system configuration is shown in Fig. 2. This method proposed in [9], overcame those problems such as transients and switching loss. In this method, primary side inverter and secondary side converter always operate in rectification mode. Transmission power is controlled by adjusting the primary side voltage and the secondary side voltage dynamically. The primary side voltage is controlled by back-boost converter connected on battery, and the secondary side voltage is controlled by DC/DC converter connected on supercapacitor. Moreover, the voltage ratio of the primary side and the secondary side is controlled to the optimal value. This control method maximized the efficiency in wide power output range. However, in the low power output range, this method cannot be used since there is a lower limit of the secondary side DC-link voltage to operate motor [10]. Then, efficient control method in low power output range is desired.

In this paper, a novel control method which is efficient in low power output range is proposed. This method is an improvement on the intermittent synchronous rectification.

II. Control method of W-IWM

A. Wireless Power Transfer system

The equivalent circuit of WPT system via magnetic resonance coupling is shown in Fig. 3. To fulfill the resonance condition, the operating frequency ω_0 is expressed as

$$\omega_0 = \frac{1}{\sqrt{L_1 C_1}} = \frac{1}{\sqrt{L_2 C_2}}. \tag{1}$$

In the resonance condition, the impedance matrix of the equivalent circuit can be expressed as

$$Z = \begin{bmatrix} R_1 & j\omega_0 L_\mathrm{m} \\ j\omega_0 L_\mathrm{m} & R_2 \end{bmatrix}. \tag{2}$$

The relationship between the voltage and the current on the primary side and the secondary side can be expressed by the following equation.

$$\begin{bmatrix} \dot{V}_1 \\ \dot{V}_2 \end{bmatrix} = Z \begin{bmatrix} \dot{I}_1 \\ -\dot{I}_2 \end{bmatrix} \tag{3}$$

In the resonance condition, the secondary side voltage $\dot{V}_2$ and the current $\dot{I}_2$ are leading $\frac{\pi}{2}$ compared to the primary side voltage $\dot{V}_1$ and the current $\dot{I}_1$. Then, they can be expressed as

$$\begin{aligned} \dot{V}_1 &= V_1 \\ \dot{V}_2 &= jV_2 \\ \dot{I}_1 &= I_1 \\ \dot{I}_2 &= jI_2 \end{aligned} \tag{4}$$

where V_1 and V_2 are the effective values of the primary side and secondary side voltage, and I_1 and I_2 are the effective values of the primary side and secondary side current, respectively. I_1 and I_2 are expressed as

$$I_1 = \frac{R_1 V_1 + \omega L_\mathrm{m} V_2}{R_1 R_2 + (\omega_0 L_\mathrm{m})^2} \tag{5}$$

$$I_2 = \frac{R_1 V_2 - \omega L_\mathrm{m} V_1}{R_1 R_2 + (\omega_0 L_\mathrm{m})^2} \tag{6}$$

The transmission power can be expressed as

$$P_\mathrm{WPT} = \dot{V}_2 \overline{\dot{I}_2} = \frac{\omega_0 L_\mathrm{m} V_1 V_2 - R_2 V_1^2}{R_1 R_2 + (\omega_0 L_\mathrm{m})^2}. \tag{7}$$

The transmission efficiency is expressed as

$$\eta_\mathrm{WPT} = \frac{\omega_0 L_\mathrm{m} V_1 V_2 - R_1 V_2^2}{\omega_0 L_\mathrm{m} V_1 V_2 + R_2 V_1^2}. \tag{8}$$

The voltage ratio at the maximum efficiency can be expressed as following equation.

$$A_{V\eta\max} = \sqrt{\frac{R_2}{R_1}} \frac{\omega_0 L_\mathrm{m}}{\sqrt{R_1 R_2 + (\omega_0 L_\mathrm{m})^2} + \sqrt{R_1 R_2}} \tag{9}$$

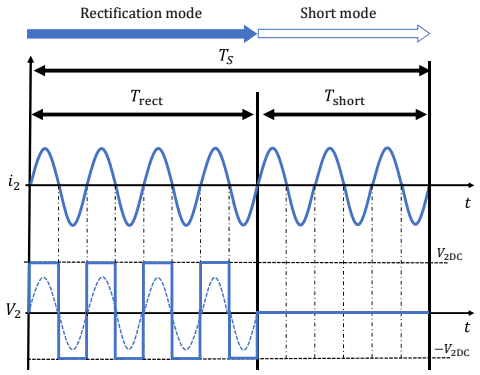

Fig. 4. Operation of secondary side converter (conventional intermittent synchronous rectification).

B. System configuration of W-IWM2

In this research, the circuit configuration of second-generation W-IWM (W-IWM2) shown in Fig. 2 is examined. In this system, WPT system using Series-Series (S-S) magnetic resonant coupling introduced in the previous chapter is employed. The primary side inverter and the secondary side converter drive each resonator at 85 kHz and it transmits power wirelessly. Those inverters are full-bridge inverter which uses SiC MOSFETs to reduce switching loss. Permanent magnet synchronous motor (PMSM) are installed on the secondary side. The motor is driven by the voltage type three phase PWM inverter. A supercapacitor for compensation, which is a feature of W-IWM2, is connected to the secondary side DC-link with a DC/DC converter.

C. Conventional intermittent synchronous rectification

Intermittent synchronous rectification [7] is proposed as a control method of WPT system under constant power load without supercapacitor. Fig. 4 shows the operation of secondary side converter. The time ratio of the rectification mode and short mode are adjusted to control transmission power corresponding to the load power. As a consequence, the secondary side DC-link voltage is stabilized.

In this method, the efficiency of the WPT system is improved compared to the two-mode control and phase shift control, since the MOSFETs of the secondary side converter are operated during rectification mode in order to achieve synchronous rectification.

However, in this method, The mode switching cycle T_s is a very short period to stabilize secondary side DC-link voltage. Then, transient current caused by mode switching does not settle sufficiently and it causes an increase in copper loss.

In order to achieve higher efficiency at low load by improved transients, the cycle of the rectification mode and the short mode should be longer, and the converter operation during mode switching should be devised.

D. Proposed intermittent synchronous rectification

The circuit configuration of W-IWM2 is shown in Fig. 2. In the proposed method, the secondary side DC-link voltage is controlled by the DC/DC converter attached to supercapacitor. The secondary side AC/DC converter controls supercapacitor's voltage. In this method, the secondary side DC-link voltage can be controlled with fast bandwidth regardless of T_s. Then, the mode switching cycle T_s can be extended without voltage ripples, and the transients caused by mode switching can be improved.

Moreover, in order to further improve transients, gradual mode switching operation is proposed as shown in Fig. 6. In this method, 3-level waveform is performed during mode switching period, and the fundamental harmonic of the secondary side voltage changes continuously. A low pass filter was applied on the pulse width command of the 3-level waveform.

The supercapacitor is connected to the DC/DC converter and it controls secondary side DC-link voltage $V_{2\mathrm{DC}}$. The block diagram is shown in Fig. 5. Inductor current of the DC/DC converter I_{SC} is controlled in the minor loop. The transfer function from I_{SC} to $V_{2\mathrm{DC}}$ is expressed as

$$P_{V_{2\mathrm{DC}}} = \frac{V_{2\mathrm{DC}}}{I_{\mathrm{SC}}} = \frac{d}{C_{\mathrm{SC}}s} \tag{10}$$

where d is a duty ratio of the DC/DC converter. For this transfer function, PI controller is designed to be a multi-root arrangement.

The voltage of the supercapacitor V_{SC} is controlled by the time ratio of the rectification mode as shown in Fig. 5. Received current of the secondary side DC-link $I_{2\mathrm{DC}}$ can be calculated as

$$I_{2\mathrm{DC}} = \begin{cases} 0 & \text{(Short mode)} \\ \frac{2\sqrt{2}}{\pi} I_2 & \text{(Rectification mode)} \end{cases} \tag{11}$$

The average of $I_{2\mathrm{DC}}$ is expressed as

$$\bar{I}_{2\mathrm{DC}} = \alpha \frac{2\sqrt{2}}{\pi} I_2. \tag{12}$$

where α is the time ratio of the rectification mode which can be expressed as

$$\alpha = \frac{T_{\mathrm{rect}}}{T_{\mathrm{rect}} + T_{\mathrm{short}}}. \tag{13}$$

The transfer function from $\Delta\bar{I}_{2\mathrm{DC}}$ to ΔV_{SC} is expressed as

$$\Delta P_{\mathrm{SC}} = \frac{\Delta V_{\mathrm{SC}}}{\Delta\bar{I}_{2\mathrm{DC}}} = \frac{V_{2\mathrm{DC}}}{2C_{\mathrm{SC}}V_{\mathrm{SC}}} \frac{1}{s} \tag{14}$$

For this transfer function, PI controller is designed to be a multi-root arrangement.

III. Simulation

We performed simulations on the proposed intermittent synchronous rectification using MATLAB/Simulink Simpower Systems. The simulation conditions are shown in Table I. In this simulation, DC to DC transmission efficiency and the transient current of the secondary side were simulated at low load, 1.3 kW. The secondary side DC-link voltage was set at 300 V which is a lower limit voltage to respond to sudden load changes. Then, the optimal primary side DC-link voltage is 302.5 V which is calculated by (9). In simulations of the

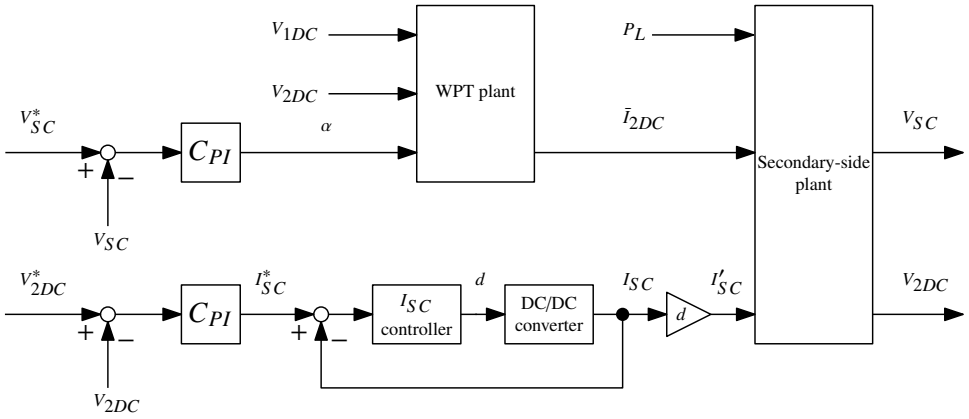

Fig. 5. Block diagram of secondary side DC-link voltage control.

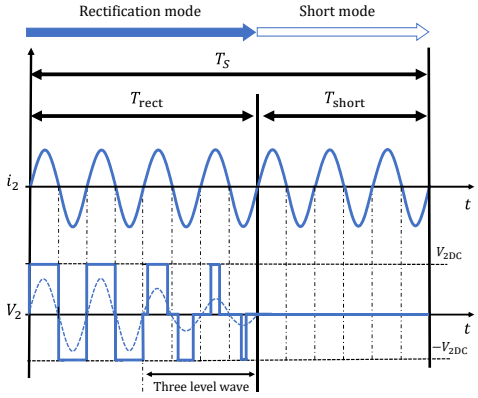

Fig. 6. Operation of secondary side converter (proposed intermittent synchronous rectification).

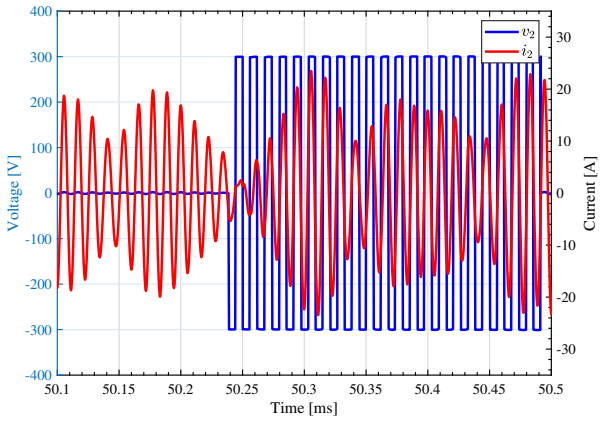

Fig. 7. Secondary side AC current and voltage of the conventional intermittent synchronous rectification ($P_{\mathrm{L}} = 1.3$ kW).

TABLE I
SPECIFICATIONS OF W-IWM SYSTEM.

Resonance frequency	86.8 kHz
Switching frequency of DC/DC converter	86.8 kHz
Switching frequency of DC/DC converter	85.0 kHz
Supercapacitor capacitance	125 F
Supercapacitor voltage reference V^*_{SC}	38 V
Primary-side coil resistance R_1	242.0 mΩ
Primary-side coil inductance L_1	259.9 μH
Secondary-side coil resistance R_2	242.0 mΩ
Secondary-side coil inductance L_2	259.9 μH
Coil gap	100 mm
Coil mutual inductance L_{m}	53 μH
Smoothing capacitance C	1100 μF
Inductance of DC/DC converter L	60.8 μF
ESR of inductor and Supercapacitor r	41.0 mΩ

conventional method, the mode switching cycle T_{S}, was set at 0.5 ms. In simulations of the proposed method, the mode switching cycle T_{S}, was set at 20 ms, and 1 kHz low pass filter was applied on the pulse width command of V_2 not to switch the mode suddenly. T_{S} was set so that the voltage ripples are comparable in those methods. Proposed method with LPF was compared to the conventional intermittent synchronous rectification and the proposed method without LPF. Simulation steps are sampled at 1.0×10^{-8} s.

A. *Transients during mode switching period*

In this section, the simulations are conducted to confirm the transient current stability. Fig. 7 shows the transient current during mode switching period of the conventional intermittent synchronous rectification. Fig. 8 shows it of the proposed method without LPF. Fig. 9 shows it of the proposed method with LPF.

It can be seen that the secondary side AC current stability is improved especially in the proposed method with LPF.

IV. EXPERIMENT

We performed experiments to confirm the effectiveness of the proposed method. The current and voltage waveform during mode switching period was measured with an oscilloscope (MSO 3024: Tektronix). Transfer efficiency is measured by a power meter (3390 POWER ANALYZER: HIOKI). Transfer efficiency is defined by the following equation.

$$\eta_{\mathrm{WPT}} = \frac{\int_{T_{\mathrm{S}}} \dot{V}_1 \overline{\dot{I}_1} dt}{\int_{T_{\mathrm{S}}} \dot{V}_2 \overline{\dot{I}_2} dt} \tag{15}$$

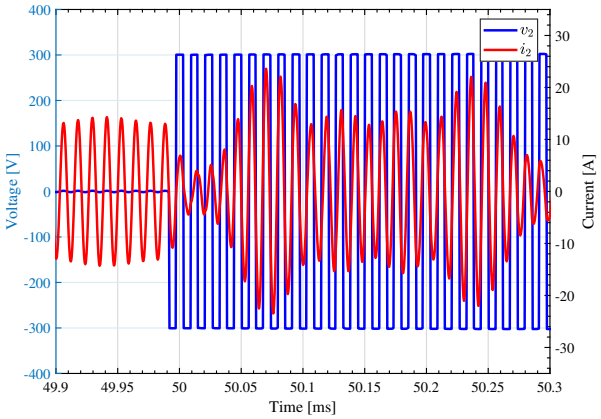

Fig. 8. Secondary side AC current and voltage of the proposed method without LPF ($P_{\mathrm{L}} = 1.3$ kW).

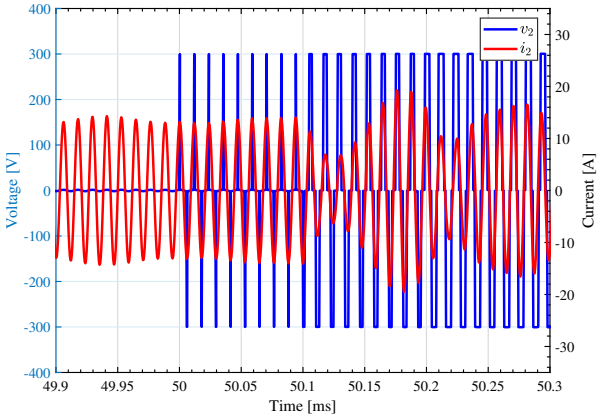

Fig. 9. Secondary side AC current and voltage of the proposed method with LPF ($P_{\mathrm{L}} = 1.3$ kW).

A. Experimental setup

The overview of the experimental setup is shown in Fig. 10. The setup consists of a primary side DC power supply, a primary side back boost converter, a primary side inverter, a transmitting and a receiving coils, a secondary side converter, a lithium ion supercapacitor, a secondary side boost converter, a voltage type three phase PWM inverter, and a PMSM. Instead of a battery, a regenerative DC power supply (pCUBE MWBFP 3-1250-J02: Myway) is used as the primary side voltage source.

B. Experimental result

1) Transient stability: The current and the voltage of the primary side and the secondary side are measured by a oscilloscope (MSO 3034: Tektronix). Fig. 11 shows the measurement results in the proposed method with LPF, Fig. 12 shows hte measurement results in the proposed method without LPF, and Fig. 13 shows the measurement results in the conventional method. Ch1, Ch2, Ch3, and Ch4 show V_1, I_1, V_2, and I_2, respectively

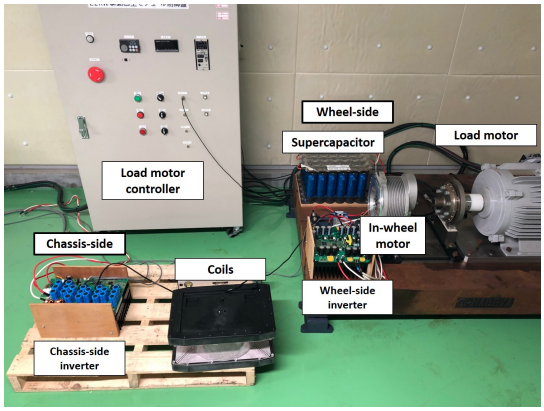

(a) Motor bench and W-IWM2.

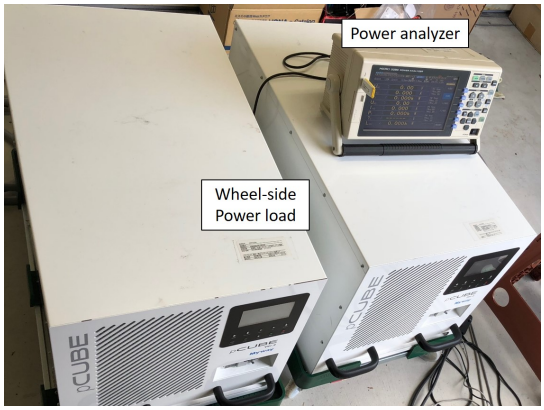

(b) Power source and power analyzer.

Fig. 10. Experimental setup.

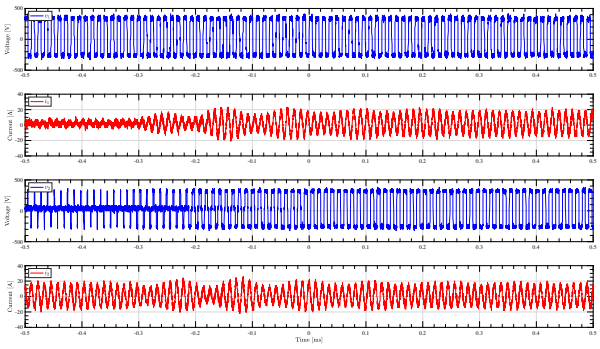

Fig. 11. Measurement results of the proposed method with LPF.($P_{\mathrm{L}} = 1.3$ kW)

It can be seen that transients stability are improved especially in the proposed method with LPF.

2) Transfer efficiency: DC to DC transmission efficiency (average value) is measured by a power meter (3390 POWER ANALYZER: HIOKI). Measurement results are shown in Fig. 14. The experimental results shows the effectiveness of the proposed method. It turns out that the proposed method with LPF is particularly effective around 2.2 kW. Aroud this range, more copper loss caused by transient current can be reduced compared to the increased switching loss.

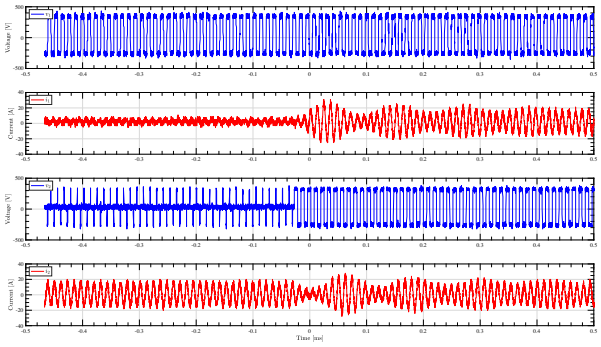

Fig. 12. Measurement results of the proposed method without LPF.($P_{\mathrm{L}} = 1.3\,\mathrm{kW}$)

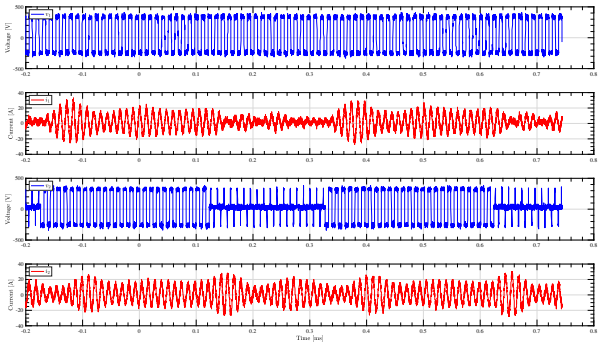

Fig. 13. Measurement results of the conventional method. ($P_{\mathrm{L}} = 1.3\,\mathrm{kW}$)

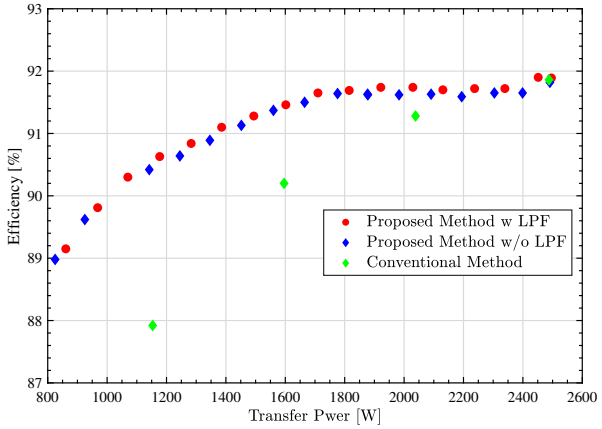

Fig. 14. Efficiency compensation of each method.

V. Conclusion

In this research, a high-efficiency operation method in the low power output range is proposed as an improvement on the intermittent synchronous rectification. In this proposed method, the mode switching cycle is lengthened and mode switching method between short mode and rectification mode are devised to improve transient stability. Although the ingenuity of the proposed mode switching method increases switching loss, it improves transients and reduces copper loss larger than increased switching loss within a specific range. In this paper, simulation and experimental results show the effectiveness of the proposed method.

VI. Acknowledgements

The contributions of Toyo Denki Seizo K.K. and NSK Ltd. are gratefully acknowledged. This work was partly supported by JSPS KAKENHI Grant Number 18H03768 and JST-Mirai Program Grant Number JPMJMI17EM, Japan.

References

[1] V.-D. Doan, H. Fujimoto, T. Koseki, T. Yasuda, H. Kishi, and T. Fujita, "Simultaneous Optimization of Speed Profile and Allocation of Wireless Power Transfer System for Autonomous Driving Electric Vehicles," *IEEJ Journal of Industry Applications*, vol. 7, no. 2, pp. 189–201, 2018. [Online]. Available: https://www.jstage.jst.go.jp/article/ieejjia/7/2/7_189/_article

[2] Y. Hori, "Research on Future Vehicle driven by Electricity and Control," *IEEE Transactions on Industrial Electronics*, vol. 51, no. 5, pp. 954–962, 2004.

[3] S. Harada and H. Fujimoto, "Range extension control system for electric vehicles based on front and rear driving force distribution considering load transfer," *(IECON) 2013-39th Annual Conference of the IEEE*, vol. 39, pp. 6626 – 6631, 2013. [Online]. Available: http://ieeexplore.ieee.org/xpls/abs_all.jsp?arnumber=6119938

[4] Y. Ikezawa, H. Fujimoto, D. Kawano, Y. Goto, Y. Takeda, and S. Koji, "Range Extension Autonomous Driving for Electric Vehicle Based on Optimal Vehicle Velocity Profile in Consideration of Cornering," *IEEJ Transactions on Industry Applications*, vol. 137, no. 1, pp. 1–9, 2016.

[5] M. Sato, G. Yamamoto, D. Gunji, T. Imura, and H. Fujimoto, "Development of Wireless In-Wheel Motor Using Magnetic Resonance Coupling," *IEEE Transactions on Power Electronics*, vol. 31, no. 7, pp. 5270–5278, 2016.

[6] K. Hata, T. Imura, and Y. Hori, "Maximum efficiency control of wireless power transfer systems with Half Active Rectifier based on primary current measurement," *2017 IEEE 3rd International Future Energy Electronics Conference and ECCE Asia, IFEEC - ECCE Asia 2017*, no. 1, pp. 1–6, 2017.

[7] M. Sato, G. Guidi, T. Imura, and H. Fujimoto, "Experimental Verification for Wireless In-Wheel Motor using Synchronous Rectification with Magnetic Resonance Coupling," *International Electric Vehicle Technology Conference & Automotive Power Electronics Japan 2016*, 2016.

[8] G. Lovison, T. Imura, H. Fujimoto, and Y. Hori, "Secondary-side-only Phase-shifting Voltage Stabilization Control with a Single Converter for WPT Systems with Constant Power Load," *IEEJ Transactions on Industry Applications*, vol. 8, no. 1, p. 66, 2018. [Online]. Available: https://www.jstage.jst.go.jp/article/ieejias/139/1/139_1/_article/-char/ja/

[9] K. Hanajiri, K. Hata, T. Imura, and H. Fujimoto, "Maximum Efficiency Operation in Wider Output Power Range of Wireless In-Wheel Motor with," in *IECON2018*, 2018.

[10] D. Tajima, K. Hanajiri, O. Shimizu, and H. Fujimoto, "Maximum E ffi ciency Operation of Wireless In-Wheel Motor Using Pulse Amplitude Modulation," in *Samcon2019*, 2019.